# 3D Numerical Modelling of a Rarefied Gas Flow in the Nearby Atmosphere around a Rotating Cometary Nucleus

Alexey N. Volkov* and German A. Lukyanov†

*Material Science and Engineering department, University of Virginia, 117 Engineer's way, Charlottesville, VA 22903, USA

†Center for Advanced Studies, St.-Petersburg State Polytechnical University, Polytechnicheskaya str., 29, 195251, St.-Petersburg, Russia

**Abstract.** A combined 3D model of a nearby atmosphere around an arbitrary rotating spherical cometary nucleus is developed. The model includes a 3D unsteady model of solar radiation absorption and heating of the nucleus material (water ice), its evaporation and condensation and a 3D quasi-stationary kinetic model of flow inside the near nucleus coma. This model can be used to predict the coma flow in conditions typical for rendezvous projects such as ESA project *Rossetta*. Calculations are carried out with the help of this model to reveal the influence of nucleus rotation on its temperature field and the flow field in the nearby atmosphere. It was found that the nucleus rotation influences significantly the nucleus temperature field and the coma flow. Vapor flow around a rotating nucleus is essentially three dimensional and differs qualitatively from the coma flow around a non-rotating nucleus.

**Keywords:** Cometary atmosphere, Rotating cometary nucleus, Heat state, Evaporation, 3D DSMC simulation
**PACS:** 96.25.Fx, 47.45.-n, 05.10.Ln

## INTRODUCTION

Modern projects of cometary studies with the help of space probes are a promising source of unique information about the nature of the solar system. Their practical realization demands preliminary understanding of basic processes in near-nucleus coma of real comets. ESA project *Rosetta* implies a meeting of the probe with the comet 67P/Churumov-Gerasimenko and landing on the surface of the nucleus. Successful accomplishment of approaching and descending of the probe and realization of the scientific program of the mission demand more detailed insight into the flow in the rarefied nearby coma than it is achieved by now. In particular, it is necessary to clarify the role of 3D effects in coma flows caused by the rotation of the nucleus, its non-homogeneity and its non-spherical shape.

A profound effect of nucleus rotation on the nucleus heat state and, in consequence, the flow in the near-by coma, was pointed out more than fifty years ago [1]. But in most computational studies only 2D axially symmetric flows in coma are considered [2]. These studies are based on simplest heat models of cometary nucleus. The formation of compression and rarefaction waves, circulation streams and other features of flows over spherical and non-spherical axially symmetric nucleus are studied with the help of such models [3]. But more realistic description of coma flows must take into account the 3D temperature field in a rotating nucleus and 3D gas flow inside a coma.

The aim of this work is to develop a combined 3D model describing the nucleus temperature field and the coma structure over an arbitrary rotating spherical nucleus. This model is used for comparative investigation of the coma over non-rotating and rotating nucleuses and the influence of the nucleus rotation is clearly revealed. For the best of authors' knowledge, the nearby cometary atmosphere is studied in a full 3D framework for the first time in this paper.

## THE MATHEMATICAL MODEL

It is assumed that the homogeneous spherical nucleus of radius $R_n$ has an ellipsoidal orbit with the period $t_s = 2\pi[(R_a+R_p)/2]^{3/2}/\sqrt{GM_s}$, where $G = 6.6720\cdot10^{-11}$ N·m$^2$/kg$^2$ is the gravitational constant, $M_s = 1.989\cdot10^{30}$ kg is the Sun's mass, $R_p$ and $R_a$ are the aphelion and perihelion distances. The nucleus' orbital motion can be calculated in the frame of reference with cartesian coordinates $Oxyz$ (Fig. 1,*a*). It is assumed that the nucleus moves anticlockwise from the top of the axis $Oz$. Position of the nucleus center $O'$ along the orbit at time $t$ can be defined by the distance between the nucleus and the Sun $r_s(t)$ and the angle $\varepsilon_s(t)$ between the direction to the Sun and the axis $Ox$. Below it

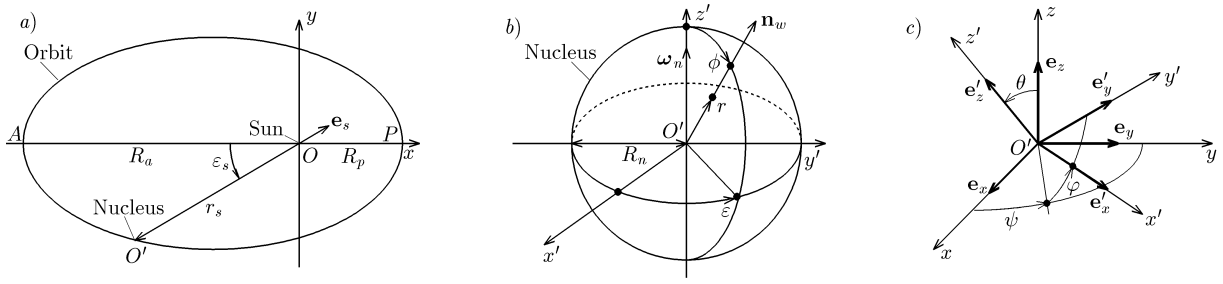


**FIGURE 1.** The coordinates which are used to calculate the orbital motion of a nucleus (*a*), its heat state (*b*) and rotation (*c*).

is assumed that at the initial time $t = 0$ the nucleus is positioned in aphelion. Then the Cauchy problem describing the varying of $r_s$ and $\varepsilon_s$ in time can be written as

$$\frac{d\varepsilon_s}{dt} = \frac{\sqrt{GM_s p}}{r_s^2}, \quad r_s = \frac{p}{1+\xi\cos\varepsilon_s}, \quad r_s(0) = R_a, \qquad \varepsilon_s(0) = 0, \tag{1}$$

where $\xi = (R_a - R_p)/(R_a + R_p)$, $p = 2R_aR_p/(R_a + R_p)$.

The nucleus temperature field is considered in the frame of reference with cartesian coordinates $O'x'y'z'$ which is fixed with respect to nucleus material (Fig. 1, *b*). The spherical coordinates $r$, $\phi$ and $\varepsilon$ are used as independent variables for the temperature field $T(r,\phi,\varepsilon,t)$ inside the nucleus. They are defined with respect to coordinates $O'x'y'z'$. The unsteady temperature field inside the nucleus is described by the heat equation

$$r^2\sin\phi\,\frac{\partial T}{\partial t} = a_n\left[\frac{\partial}{\partial r}\left(r^2\sin\phi\,\frac{\partial T}{\partial r}\right) + \frac{\partial}{\partial\phi}\left(\sin\phi\,\frac{\partial T}{\partial\phi}\right) + \frac{\partial}{\partial\varepsilon}\left(\frac{1}{\sin\phi}\,\frac{\partial T}{\partial\varepsilon}\right)\right], \tag{2}$$

where $a_n = \kappa_n/(\rho_n c_n)$, $\rho_n$, $c_n$ and $\kappa_n$ are the density, the specific heat and the heat conduction of the nucleus material.

The boundary condition at the nucleus surface is the equation of energy balance between the flux of the Sun's radiation absorbing by the nucleus, the heat conduction flux describing heat propagation in the nucleus, the flux of radiation emitted by the nucleus according to the Stefan-Boltzmann law and the energy flux due to evaporation

$$(1-A_n)I_0\left(\frac{r_0}{r_s}\right)^2\cos\gamma = \kappa_n\left.\frac{\partial T}{\partial r}\right|_{r=R_n} + \beta_n\sigma T_w^4 + L_n\psi_w, \tag{3}$$

where $A_n$ is the nucleus albedo, $I_0 = 1360.4$ W/m$^2$ is the Sun's radiation intensity at the distance $r_0 = 1.496\cdot 10^{11}$ m (1 a.u.), $\beta_n$ is the emissivity factor of the nucleus surface, $\sigma$ is the Stefan-Boltzmann constant, $L_n$ is the specific latent heat of evaporation, $\psi_w$ is the mass flux density of the evaporated material (local gas production rate), $T_w$ is the surface temperature and $\gamma$ is the zenith angle ($\cos\gamma = \mathbf{e}_s\cdot\mathbf{n}_w$ if $\mathbf{e}_s\cdot\mathbf{n}_w > 0$, $\cos\gamma = 0$ otherwise, $\mathbf{e}_s$ is the unit vector directed from the nucleus center $O'$ to the Sun and $\mathbf{n}_w$ is the unit normal to the surface pointed outward from the nucleus).

The mass flux density $\psi_w$ in (3) can be represented in the form $\psi_w = \psi_w^+ - \psi_w^-$, where $\psi_w^+$ and $\psi_w^-$ are the mass flux densities of molecules emitting and absorbing by the nucleus surface

$$\psi_w^+(R_n\mathbf{n}_w,t) = m\int\limits_{\mathbf{v}'\cdot\mathbf{n}_w>0}\mathbf{v}'\cdot\mathbf{n}\,f'(R_n\mathbf{n}_w,\mathbf{v}',t)d\mathbf{v}', \qquad \psi_w^-(R_n\mathbf{n}_w,t) = -m\int\limits_{\mathbf{v}'\cdot\mathbf{n}_w<0}\mathbf{v}\cdot\mathbf{n}\,f'(R_n\mathbf{n}_w,\mathbf{v}',t)d\mathbf{v}'. \tag{4}$$

Here $\mathbf{v}'$ and $f'(\mathbf{r},\mathbf{v}',t)$ are the velocity vector of a vapor molecule and the velocity distribution function normalized by the vapor concentration $n$ ($\int f'd\mathbf{v}' = n$) in the frame of reference $O'x'y'z'$ ($\mathbf{v}' = \mathbf{v} - R_n\boldsymbol{\omega}_n\times\mathbf{n}_w$, where $\mathbf{v}$ and $\boldsymbol{\omega}_n$ are the velocity vector of a molecule and the angular velocity of the nucleus in the frame of reference $Oxyz$).

In order to calculate $\psi_w$ it is assumed that: (1) the Hertz-Knudsen model can be used to describe evaporation of the nucleus material; (2) the evaporation and condensation coefficients are equal to unity; (3) the equilibrium pressure of vapor $p_e(T)$ as a function of its temperature $T$ is described by the Clausius-Clapeyron equation $p_e(T) = p_0\exp(-T_0/T)$ ($p_0$ and $T_0$ are constants for cometary ice) and (4) fraction $1 - f_n$ of the nucleus surface is coated by the non-volatile material. Then the distribution function of evaporating molecules is equal to

$$\text{at } \mathbf{r} = R_n\mathbf{n}_w,\ \mathbf{v}'\cdot\mathbf{n}_w > 0: \quad f'(\mathbf{r},\mathbf{v}',t) = f_n\frac{p_e(T_w)}{k_BT_w}\left(\frac{m}{2\pi k_BT_w}\right)^{3/2}\exp\left(-\frac{m(\mathbf{v}')^2}{2k_BT_w}\right), \tag{5}$$

where $m$ is the mass of vapor molecules, $k_B$ is the Boltzmann's constant. Substituting (5) into the first relation in (4) one can find $\psi_w^+ = f_n p_e(T_w)/\sqrt{2\pi k_B T_w/m}$. The distribution function $f'(\mathbf{r},\mathbf{v}',t)$ at $\mathbf{v}'\cdot\mathbf{n}_w < 0$ and the "back" flux $\psi_w^-$ corresponding to molecules condensed at the surface are determined as a part of kinetic problem for the coma flow.

The heat problem for equation (2) is solved with the homogeneous initial condition

$$\text{at } t = 0: \quad T(r,\phi,\varepsilon,0) = T^*. \tag{6}$$

The initial temperature $T^*$ of the nucleus is assumed to be equal to the "balance" temperature of the surface at the zenith point in perihelion, which is found from the equation $(1-A_n)I_0(r_0/R_p)^2 = \beta_n\sigma(T^*)^4 + L_n\psi_w^+(T^*)$.

It is assumed that the nucleus rotates over the axis $O'z'$ with the period of revolution $t_n$. The Euler's angles $\psi$, $\theta$ and $\varphi$ are used in order to describe the nucleus rotation, see Fig. 1, *c*. Then the rotation is defined by relations $\psi(t) = \psi^0$, $\theta(t) = \theta^0$, $\varphi(t) = \varphi^0 + 2\pi t/t_n$, where $\psi^0$ and $\theta^0$ specify direction of the rotational axis $O'z'$ with respect to the frame of reference $Oxyz$ and for the initial condition (6) a solution of the equation (2) does not depend on $\varphi^0$.

The model (2)-(3) describing the heat state of the cometary nucleus belongs to the class of heat models known as the slow rotator models [5]–[9]. But in cited papers an approximate 1D heat equation (or 1D equations describing the heat state, evaporation and diffusion of vapor in the porous nucleus) is solved instead of 3D heat equation (2).

The problem (1)-(6) is solved numerically by the finite-difference scheme with second order of approximation in time and spatial coordinates. This scheme is similar to the scheme described in paper [4] for 2D axially symmetric heat problem. Initially, the problem (1)-(6) is solved with $\psi_w^- = 0$ for a time $t_* \gg t_s$. Then the temperature field $T(r,\phi,\varepsilon,t_*)$ at time $t_*$ is used as an initial condition for simulation of the coma vapor flow.

It is assumed that the coma consists of water vapor which is considered as a rarefied gas. It means that only binary collisions are taken into account. Every vapor molecule has 3 translational and 3 rotational degrees of freedom. The current state of molecule "i" is specified by its position vector $\mathbf{r}_i$, its translational velocity vector $\mathbf{v}_i$ and its rotational energy $\varepsilon_{ri}$. Transformation of these state variables during a binary collision is described by the VHS model coupled with the Larsen-Borgnakke model (see [10]). The total collision cross section for a pair of molecules with velocities $\mathbf{v}_i$ and $\mathbf{v}_j$ are defined by the formula $\sigma_t(\mathrm{g}) = \pi d_0^2(\mathrm{g}/\mathrm{g}_0)^{2\varpi-1}$, where $\mathrm{g} = |\mathbf{v}_j - \mathbf{v}_i|$ is the molecules' relative velocity, $\varpi$ is the exponent in the temperature law for the gas viscosity, $d_0$ and $\mathrm{g}_0$ are some "reference" constants.

Molecules translational velocities after a collision can be found in the same way as for hard spheres, i.e. $\mathbf{v}_i^* = (1/2)(\mathbf{v}_i + \mathbf{v}_j - \mathrm{g}^*\mathbf{d})$, $\mathbf{v}_j^* = (1/2)(\mathbf{v}_i + \mathbf{v}_j + \mathrm{g}^*\mathbf{d})$, where $\mathrm{g}^*$ is the relative velocity after the collision and $\mathbf{d}$ is the isotropic unit vector. Here and after post-collisional values of any parameters are denoted by the superscript "$*$".

In the Larsen-Borgnakke model, it is assumed that inelastic collisions take place with a some probability $P_r$. If collision is elastic then $\mathrm{g}^* = \mathrm{g}$, $\varepsilon_{ri}^* = \varepsilon_{ri}^*$ and $\varepsilon_{rj}^* = \varepsilon_{rj}^*$. If collision is inelastic then the post-collisional values of the relative translational energy $\varepsilon_t^* = m(g^*)^2/4$ and the rotational energy $\varepsilon_{ri}^*$ of molecule $i$ are distributed with densities

$$F(\varepsilon_t^*) = \frac{\Gamma(11/2-\varpi)}{\Gamma(5/2-\varpi)\Gamma(3)\varepsilon}\left(\frac{\varepsilon_t^*}{\varepsilon}\right)^{3/2-\varpi}\left(1-\frac{\varepsilon_t^*}{\varepsilon}\right)^2, \quad F(\varepsilon_{ri}^*) = \frac{\Gamma(3)}{[\Gamma(3/2)]^2\varepsilon_r^*}\left(\frac{\varepsilon_{ri}^*}{\varepsilon_r^*}\right)^{1/2}\left(1-\frac{\varepsilon_{ri}^*}{\varepsilon_r^*}\right)^{1/2}, \tag{7}$$

where $\varepsilon = m\mathrm{g}^2/4 + \varepsilon_{ri} + \varepsilon_{jr}$ is the total energy of the molecular pair, $\varepsilon_r^* = \varepsilon - \varepsilon_t^*$, $\Gamma(x)$ is the gamma function. Then $g^* = 2\sqrt{\varepsilon_t^*/m}$ and $\varepsilon_{rj}^*$ can be calculated from the energy conservation law: $\varepsilon_{rj}^* = \varepsilon_r^* - \varepsilon_{ri}^*$.

The direct simulation Monte Carlo method is applied to calculate the flow of water vapor around the nucleus. In calculations, the Bird's NTC scheme of the DSMC method is used [10]. Computation of the nucleus temperature and the coma flow are carried out with the help of parallel computational code. The computational domain for the DSMC simulation is a cube with the facet size $L_{c.d.}$ (in calculations described below $L_{c.d.} = 10R_n$). The outer boundary of the computational domain is assumed to be located in the region of the supersonic flow, so that the flux of molecules moving into the computational domain through this boundary is neglected. The nucleus is positioned in the center of the cube. The distribution (5) is used as the boundary condition for translational velocities of evaporated atoms. The rotational energy $\varepsilon_{ri}$ of evaporating atoms at the surface is found from the equilibrium Boltzmann's distribution [10].

## RESULTS AND DISCUSSION

Calculations are carried out for the following set of governing parameters (see [2, 3]): $\rho_n = 900$ kg/m$^3$, $c_n = 1000$ J/(kg·K), $\kappa_n = 2.2$ W/(m·K), $A_n = 0.05$, $\beta_n = 0.9$, $f_n = 0.8$, $k_B/m = 460$ J/(kg·K), $L_n = 2.4\cdot10^6$ J/kg, $p_0 = 3.56\cdot10^{12}$ Pa, $T_0 = 6141$ K, $d_0 = 6.15\cdot10^{-10}$ m, $\varpi = 1.1$, $g_0 = 822.4$ m/s, $P_r = 1$. Only two cases are considered below. Case I corresponds to the non-rotating nucleus and case II corresponds to the rotating nucleus with $t_n = 200$ h,

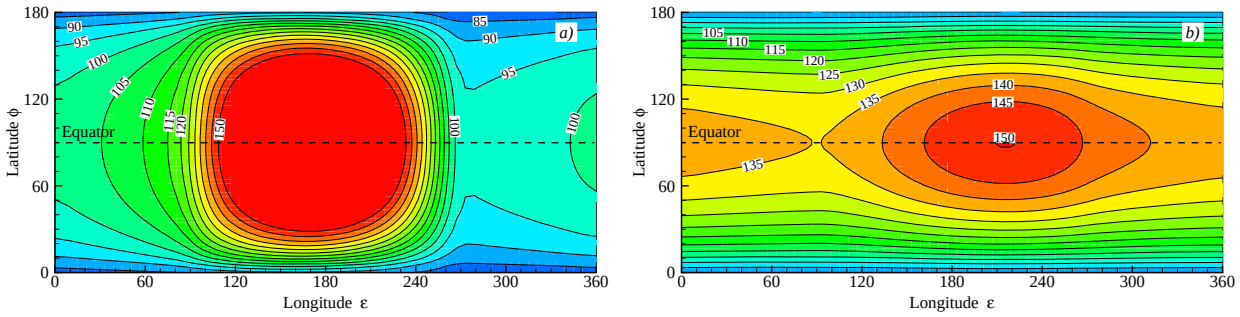


**FIGURE 2.** Contours of the constant temperature $T_w$ at the surface of non-rotating (*a*) and rotating (*b*) cometary nucleuses. The temperature difference between nearest contours is equal to 5 K. The longitude $\varepsilon = 180^\circ$ corresponds to the direction to the Sun.

$\psi^0 = \theta^0 = 0$ which means that the rotational axis $O'z'$ is perpendicular to the orbit's plane. In both cases $R_n = 500$ m, $R_a = R_p = 4.5$ a.u. ($t_s \approx 83683$ h, $T^* \approx 178.9$ K), the angle $\varphi^0$ is assumed to be equal to $180^\circ$, $t_* = 10t_s$.

Temperature fields $T_w$ at the surface of the non-rotating and rotating nucleuses are shown in Fig. 2. Both fields are symmetric with respect to equator ($\phi = 90^\circ$). The temperature field at the surface of the non-rotating nucleus in Fig. 2, *a* is also approximately symmetric with respect to the direction to the Sun ($\varepsilon = 180^\circ$). A little asymmetry of the temperature field with respect to direction $\varepsilon = 180^\circ$ arises as a result of the orbital motion of the nucleus because different heat conditions take place in the regions of the nucleus surface which move from the shadow to the illuminated surface and in the opposite direction. The maximal temperature of the surface is $\approx 177$ K, the temperature at the shadow part of the surface is $\approx 100$ K and the temperature in the near-pole regions is $\approx 77$ K.

The temperature field $T_w$ at the surface of the rotating nucleus in Fig. 2, *b* is rather different. The temperature field for the rotating nucleus is more asymmetric with respect to the direction to the Sun. The maximal temperature at the surface is $\approx 150$ K and it is much less than for the non-rotating nucleus. The temperature gradients in the longitudinal direction $\varepsilon$ for the rotating nucleus are also much less as compared with the non-rotating nucleus.

The difference in temperature fields results in corresponding difference of the local gas production rate $\psi_w$ at the surfaces of the non-rotating and rotating nucleuses. Because the maximal surface temperature of non-rotating nucleus is much higher, the maximal values $\psi_{w\max}$ of the gas production rate $\psi_w$ and the integral gas production rate $\Psi_n$ (gas production rate for the whole nucleus) for the non-rotating nucleus are also higher as compared with the rotating nucleus: $\psi_{w\max} \approx 3 \cdot 10^{-6}$ kg/(s·m$^2$), $\Psi_n \approx 0.68$ kg/s for the non-rotating nucleus and $\psi_{w\max} \approx 7 \cdot 10^{-9}$ kg/(s·m$^2$), $\Psi_n \approx 0.0018$ kg/s for the rotating one.

The changes in the temperature field and the gas production rate due to the nucleus rotation result in qualitative changes in the flow field structure of the nearby nucleus atmosphere. The vapor concentration fields $n(x,y)$ in the equatorial cross-section of the coma are shown in Fig. 3 for the non-rotating (*a*) and rotating (*b*) nucleuses. One can see that the concentration field for the rotation nucleus is highly asymmetric with respect to the direction to the Sun. Nucleus rotation also results in decreasing of vapor concentration in the coma, especially at the illuminated part of the nucleus surface where the concentration is in two decimal orders less as compared with the case of the non-rotating nucleus. It means that flow conditions at the illuminated surface of the non-rotating and rotating nucleuses differ significantly. The minimal local Knudsen number $\lambda/R_n$ ($\lambda$ is the local value of the molecules mean free path) in the coma over the non-rotating nucleus is less then 0.001 and transitional flow takes place near the illuminated surface. For the rotating nucleus the minimal local Knudsen number is $\approx$0.5 and this corresponds to almost free molecular flow.

At the surface of the rotating nucleus the minimal vapor concentration is realized in near-pole regions (it is in $10^4$ times less than the maximal concentration) but the concentration field is rather homogeneous along the equator where the ratio between maximal and minimal concentration is less than 100. On the contrary, the vapor distribution along the equator at the non-rotating nucleus is highly inhomogeneous and the ratio of the maximal and minimal concentrations in the illuminated and shady regions is more than $10^5$.

Streamlines patterns shown in Fig. 4 and 5 also differ qualitatively for the non-rotating and rotating nucleuses. In these patterns, all streamlines are 3D curves because all three components of the gas macroscopic velocity field are used in order to calculate them. Generally, flow fields have 3D nature in both cases. But for the non-rotating nucleus the flow field is rather close to the 2D axially symmetric flow (Fig. 4, *a*). This flow is characterized by large differences in vapor concentration and pressure near the illuminated and shady parts of the nucleus surface. This results in the turn

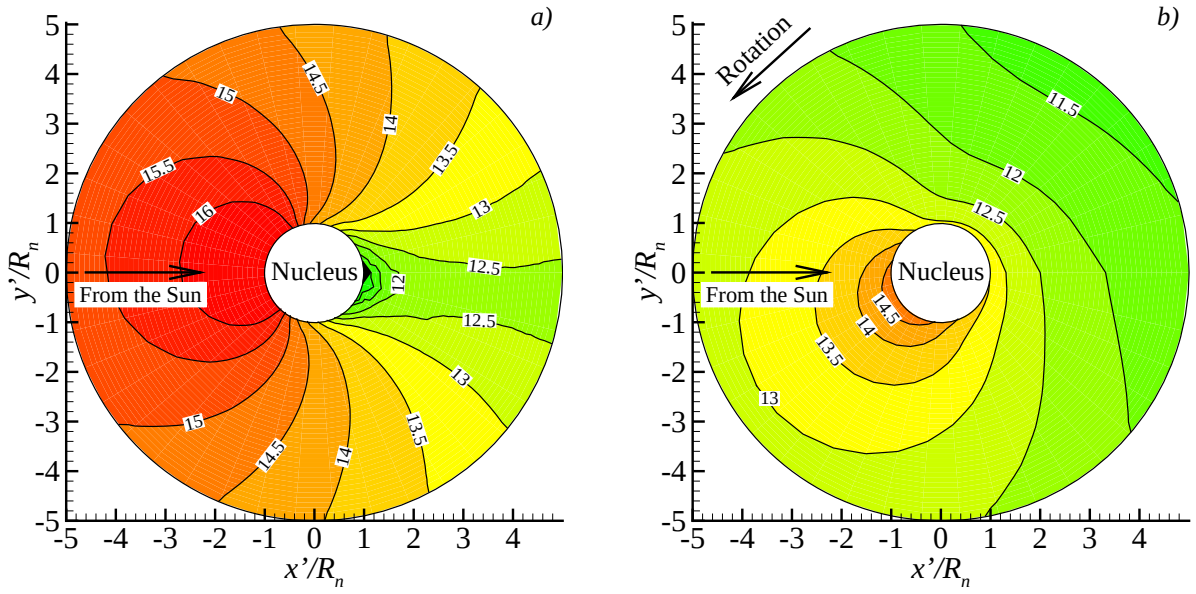


**FIGURE 3.** Contours of the constant vapor concentration $n$ in the equatorial cross-section $\theta = 90^\circ$ ($z' = 0$, see Fig. 2, *b*) of the coma over the non-rotating (*a*) and rotating (*b*) cometary nucleuses. Values of $\lg(n)$ are shown along contours. The axis $Ox'$ points from the Sun.

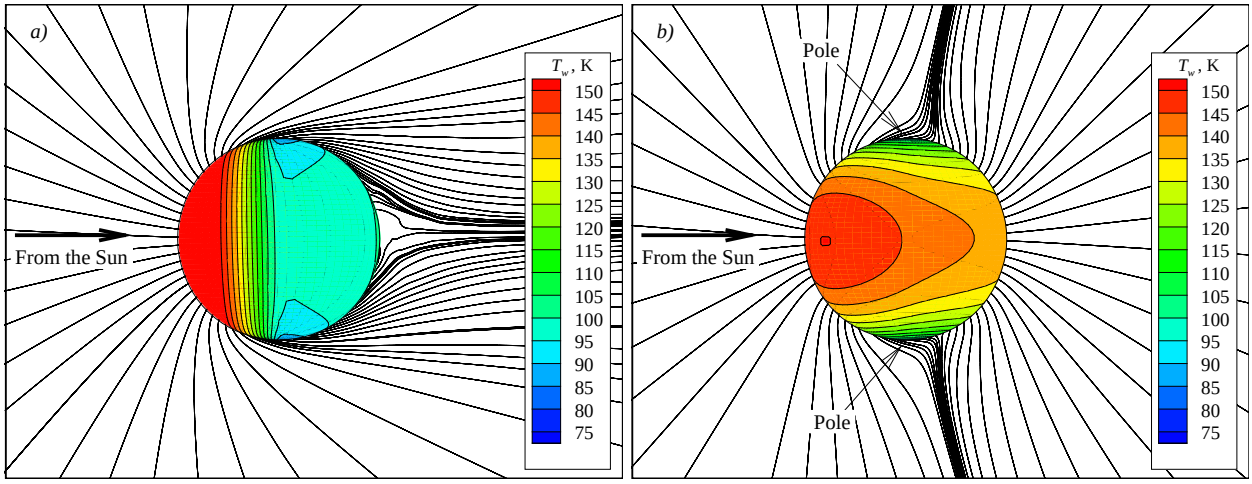


**FIGURE 4.** Surface temperature contours and streamlines patterns in the coma around the non-rotating (*a*) and rotating (*b*) cometary nucleuses. Streamlines start from the surface of the nucleus in the plane $O'x'z'$ ($\varepsilon = 0$ and $\varepsilon = 180^\circ$, see Fig. 1, *b* and *c*) at the time when the axis $O'x'$ points to the Sun.

of the vapor flow from the illuminated to the shady part of the surface. The flow at the shady part of the surface is formed by the gas evaporated from the thin surface ring near the boundary between the illuminated and shady regions. This flow structure is similar to the axially symmetric flow over the non-rotating cometary nucleus studied in [2, 3].

The flow field around the rotating nucleus (Fig. 4, *b* and 5) is essentially three dimensional. The flow structures of the expanding vapor in the orbital plane (it coincides with the nucleus equatorial cross-section) and in the perpendicular plane $Ox'z'$ (containing the direction to the Sun $\mathbf{e}_s$ and the rotational axis $O'z'$) are quite different. The flow in the orbital plane (Fig. 5, *a*) is similar to the flow from the spherical source. In the plane $O'z'$ the flow turns from the equatorial region to poles. The spatial flow over the rotating nucleus is demonstrated in Fig. 5, *b* (streamlines are shown in the figure for a semi-sphere only). A rarefied "jet" (the pressure is quite low in this region) is formed near the pole. In the

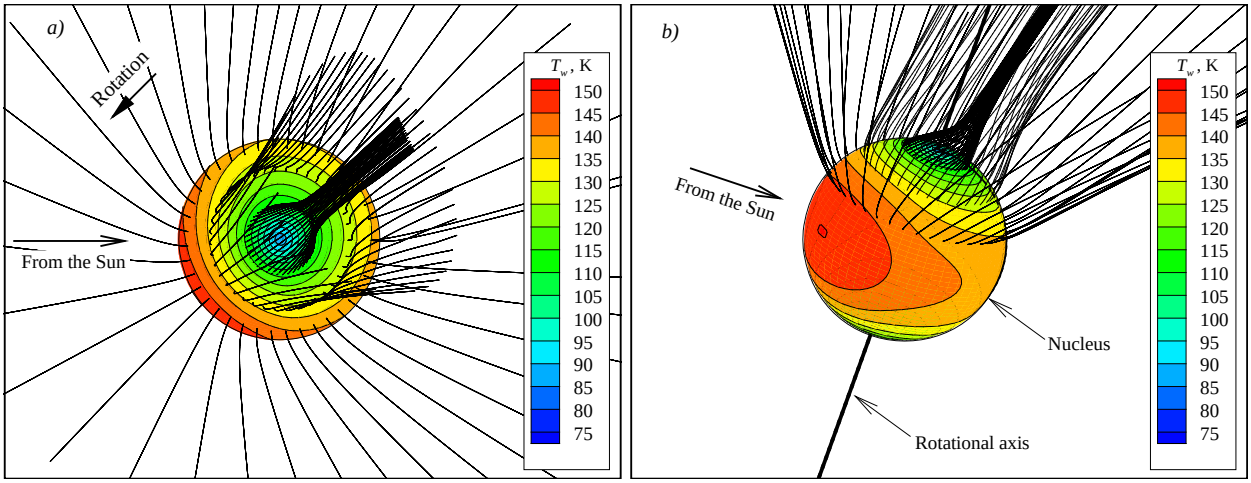


**FIGURE 5.** Surface temperature contours and streamlines patterns in the coma around the rotating cometary nucleus. *a*, the view from the top of the rotational velocity vector $\omega_n$ (axis $Oz'$); *b*, the axonometric view of the same pattern.

orbital plane (Fig. 5, *a*) this jet flows in the direction rotated at the angle $\approx 45^\circ$ to the direction to the Sun.

Therefore, in both cases one can see the turn of the vapor flow in the direction from the high pressure regions to the regions with lowest pressure. For the non-rotating nucleus large region with very low pressure is realized near the point at the shady surface which is opposite to the zenith point. On the contrary, the minimal pressure at the surface of rotating nucleus is realized in the near-polar regions. This is the main reason for the qualitative difference between flows over the non-rotating and rotating nucleuses.

## CONCLUSION

The 3D combined model of the cometary nucleus heat state and the coma flow is developed and applied for modelling of the coma structure around a rotating spherical nucleus. Computational results clearly demonstrate the qualitative difference in the coma structure for the non-rotating and rotating nucleuses. The flow over the rotating nucleus is found to be essentially three dimensional. Authors plan to use the developed model for systematic investigation of coma flows around rotating nucleuses. The computational model can be also used as a basis for further studies of the coma structure around real non-spherical and non-homogeneous cometary nucleuses.

## ACKNOWLEDGMENTS

This work is supported by the Russian Foundation for Basic Research (grant No. 04-01-00061).

## REFERENCES

1. P. L. Whipple, *Astrophys. J.* **III**, 375–394 (1950).
2. J. F. Crifo, G. A. Loukianov, A. V. Rodionov, and V. V. Zakharov, *Icarus* **156**, 249–268, (2002); *Icarus* **163**(2), 479–503 (2003).
3. G.A. Lukyanov, V.V. Zakharov, A.V. Rodionov, and J.F. Crifo, in *Proc. of the 24th RGD Symposium, American Institute of Physics*, Melville, New York, 2004, pp. 331–336.
4. A. N. Volkov, *Matematicheskoe modelirovanie* **17**(8), 5–14, in Russian (2005).
5. J. Benkhoff, *Planet. Space Sci.* **47**, 735–744 (1999).
6. A. Enzian, J. Klinger, G. Schwehm, and P. R. Weissman, *Icarus* **138**, 74–84 (1999).
7. W. H. Julian, M. N. Samarasinha, and M. J. S. Belton, *Icarus* **144**, 160–171 (2000).
8. M. Cohen, D. Prialnik, and M. Podolak, *New Astronomy* **8**, 179–189 (2003).
9. B. J. R. Davidsson, and P. J. Gutiérrez, *Icarus* **176**, 453–477 (2005).
10. G. A. Bird, *Molecular Gas Dynamics and the Direct Simulation of Gas Flows*, Clarendon Press, Oxford, 1994.